RSC Advances

PAPER

View Article Online
View Journal | View Issue

Cite this: *RSC Adv.*, 2025, **15**, 13364

Reaction of polarizing agent Ox063 with pyruvic acid under standard sample preparation protocol for dissolution dynamic nuclear polarization†

Benoit Driesschaert *[ab] and Megan M. Holloway [ab]

Received 24th February 2025
Accepted 15th April 2025

DOI: 10.1039/d5ra01347j

rsc.li/rsc-advances

Dynamic nuclear polarization is a technique that significantly enhances signal intensity in nuclear magnetic resonance spectroscopy and imaging. In a DNP experiment, a sample of interest is doped with a radical, and microwaves are applied in a strong magnetic field, leading to an increase in nuclear spin polarization. Notably, the potential reactions between the sample and the polarization agent are rarely considered. Hyperpolarized ^{13}C magnetic resonance spectroscopy (MRS) is currently used in clinical trials for various diseases. Herein, we demonstrated that with one of the mostly used DNP systems, pyruvic acid, hyperpolarized with the trityl radical Ox063, the alcohol moieties of the radical undergo esterification during sample preparation, leading to the formation of pyruvate esters on the radical, and that Ox063 has a half-life of ~30 min in pyruvic acid at room temperature. The biological and physicochemical properties of these derivatives have not yet been studied.

Dynamic nuclear polarization (DNP) is a powerful technique that significantly enhances the signal-to-noise ratio in nuclear magnetic resonance (NMR) and magnetic resonance imaging (MRI) by transferring polarization from unpaired electrons to nuclei. In pre-clinical and clinical research, dissolution DNP (dDNP) enables real-time *in vivo* metabolic imaging.[1] In dDNP experiments, a ^{13}C-enriched metabolite is mixed with a stable radical polarizing agent (PA) in a glass-forming solvent. Gadolinium(III) complexes are sometimes added to improve the polarizing efficiency.[2] The sample is then frozen to cryogenic temperature (1.2–5 K) and polarized by applying microwave radiation under a strong external magnetic field ($3.3 < B_0 < 10$ T). After sufficient polarization build-up, $P(^{13}C) > 30\%$, the sample is rapidly dissolved using a superheated solvent or buffer and then quickly injected *in vivo* to minimize polarization loss, and magnetic resonance spectroscopy (MRS) is performed to gain real-time spatial metabolic information.[3,4] This technique is progressing rapidly and are used in multiple clinical trials that are currently being conducted for multiple diseases.[5] Although numerous ^{13}C-enriched biologically relevant metabolites have been used, hyperpolarized pyruvic acid remains the most popular one thus far because of its long T_1 relaxation time constant, its efficient polarization, and, most importantly, its central role in cellular metabolism.[1,6–19] Among the PAs, the stable radical Ox063 (Fig. 1) has been one of the most used PA. Its high stability, water solubility, and narrow EPR single line make it an ideal PA for polarizing ^{13}C-enriched biologically relevant species. In pre-clinical settings, Ox063 is injected together with the hyperpolarized ^{13}C agent owing to its non-toxic properties (LD_{50} mice = 8 mmol kg^{-1})[20,21] and fast clearance.[22,23] Notably, Ox063 and its deuterated analog, Ox063-d_{24} (also known as Ox071), have been extensively used as systemic molecular oxygen sensors for electron paramagnetic resonance (EPR) and Overhauser-enhanced MRI oxygen mapping in multiple animal models, showing high biocompatibility.[24,25]

Surprisingly, despite the large body of literature on DNP method optimization, DNP mechanistic study, or biomedical/medical applications, the potential interactions/reactions between the PA, the solvents, the analyte to be hyperpolarized, and other components of the sample during sample preparation were too rarely considered, and often, there have been the consequence of unexpected results such as the lack of NMR enhancement with Ox063 or 4-oxo-TEMPO in presence of silver ion.[26] The formation of aggregates of Ox063 at high concentrations has been discussed and shown to have significant consequences on DNP signal enhancement and mechanisms.[27] The hyperpolarization of [1-^{13}C]pyruvic acid with the Ox063 radical being the most popular dDNP system, we investigated the potential reaction between these two molecules. Based on our experience in the synthesis and derivatization of Ox063 and Ox063-d_{24} radicals,[28–30] we hypothesized that Ox063 could react with pyruvic acid *via* Fischer esterification. Ox063 exhibits 12 primary alcohol moieties that could react with the carboxylic acid of pyruvic acid, leading to an Ox063-pyruvate ester (Fig. 1).

[a]*Department of Pharmaceutical Sciences, School of Pharmacy, West Virginia University, Morgantown, WV, 26505, USA. E-mail: benoit.driesschaert@hsc.wvu.edu*
[b]*In Vivo Multifunctional Magnetic Resonance Center, West Virginia University, Morgantown, WV, USA*

† Electronic supplementary information (ESI) available. See DOI: https://doi.org/10.1039/d5ra01347j

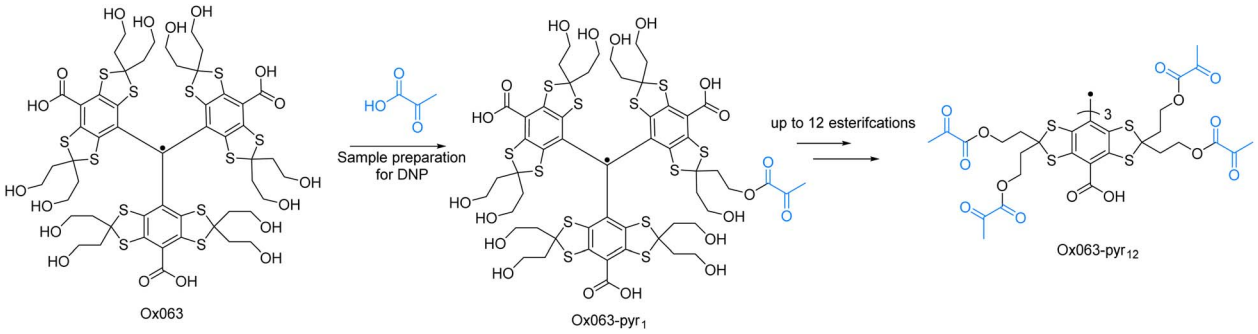

Fig. 1 Structure of the Ox063 radical, and its hypothesized reaction with pyruvic acid leading to Ox063-pyruvate esters.

The significance of these potential derivatives may be high because their biological effects have not been tested. More broadly, when PAs are compared or when DNP enhancement is rationalized based on molecular structures, the alteration of the molecules of the sample constituents could lead to false conclusions.[31]

The most common protocol for sample preparation of pyruvic acid for hyperpolarization is the dissolution of Ox063 radical at 15–20 mM in neat [1-^{13}C]pyruvic acid (~14 M) with or without Gd^{3+} chelates.[6–19] The sample is usually vortexed and/or sonicated for a few minutes. Aliquots not directly used are stored long-term at low temperatures (−80 °C to 4 °C). To verify our hypothesis, Ox063 was mixed at 15 mM in neat pyruvic acid at room temperature (25 °C), and the mixture was analyzed by reverse-phase HPLC/MS.

The first chromatogram in Fig. 2A (in black) recorded after ~5 min of sonication and vortex mixing, which was required to reach a homogeneous solution, shows that in addition to the peak of Ox063 with a retention time of 1.7 min, additional smaller peaks at 4–5 minutes are also present. The UV-vis spectrum of the peak at 4.3 min (Fig. 2B) is almost identical to the spectrum of Ox063, indicating a trityl radical structure, while the MS spectrum reveals an m/z of 1430 consistent with the structure of Ox063-pyr$_1$ (Fig. 2C and 1 for the structure). The other peaks correspond to Ox063 with multiple pyruvate esters. When the solution was left at room temperature and analyzed by HPLC/MS over time, the peak of Ox063 progressively

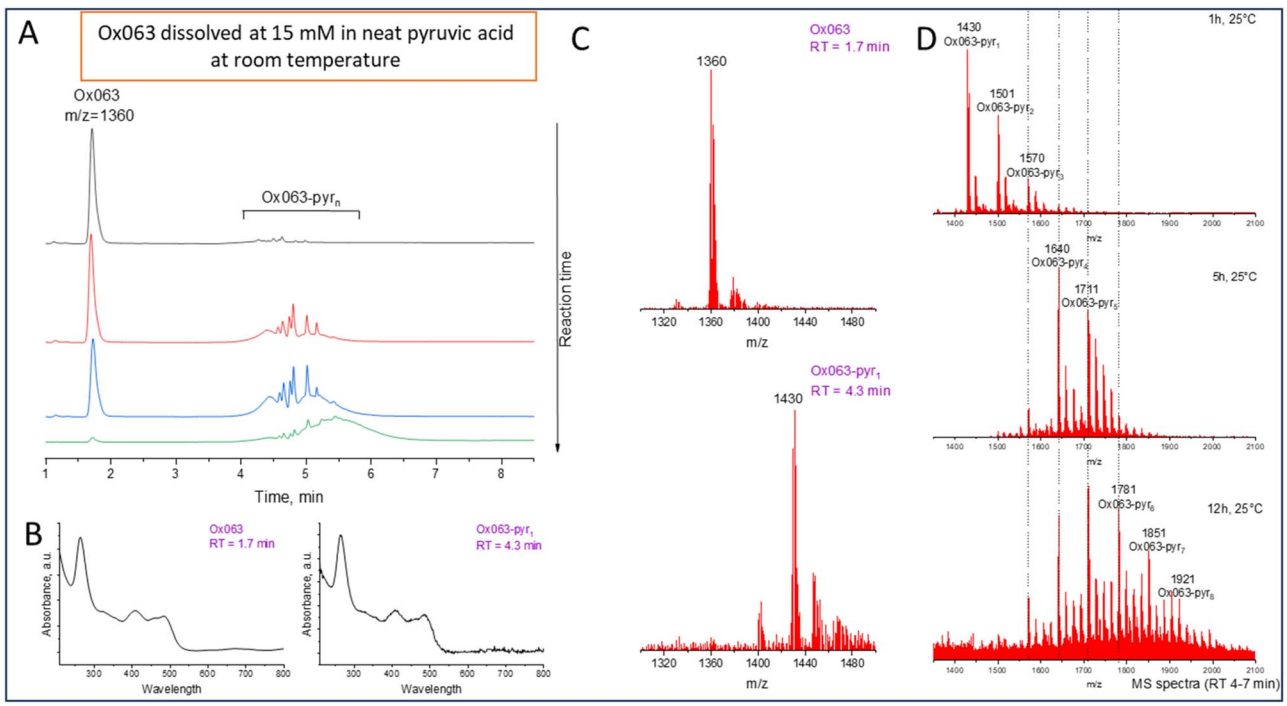

Fig. 2 (A) HPLC chromatograms at 485 nm of Ox063 (15 mM) dissolved in neat pyruvic acid (~14 M) at room temperature after ~5 min, 40 min, 65 min, and 3 h. (B) UV spectra of the peak at 1.7 min (Ox063) and 4.3 min (Ox063-pyr$_1$) for the first chromatogram (5 min of reaction). (C) MS spectra of the peak at 1.7 min (Ox063) and 4.3 min (Ox063-pyr$_1$) for the first chromatogram (5 min of reaction). (D) MS spectra integrated over a retention time window of 4–7 min of the reaction after 1, 5, and 12 h at 25 °C.

decreased while the peaks of the Ox063-pyruvate esters (Ox063-Pyr_n, $1 < n < 12$) increased. Because of the high number of possible isomers, as the reaction progresses, the number of peaks increases dramatically, and they all merge into a broad peak. As a result, MS spectra were extracted from a window of retention time from 4 to 7 min. As shown in Fig. 2D, after one hour of reaction, the m/z values corresponding to 1, 2, and 3 pyruvate esters of Ox063 were the most intense. This distribution shifts over time to higher numbers of pyruvate esters.

To obtain more quantitative information, reaction kinetics were performed at 20, 25, 30, and 35 °C. Ox063 was mixed at 15 mM in neat pyruvic acid in an HPLC vial. The temperature of the HPLC sample manager was set to the desired temperature, and chromatograms were recorded over time to determine the remaining concentration of Ox063. Fig. 3 shows the kinetics and fitting using a pseudo-first-order integrated rate law (see Fig. S1 for replication†).

Table 1 summarizes the kinetic parameters. The half-life of Ox063 in pyruvic acid is as low as 12 ± 4 minutes at 35 °C. Some DNP sample preparation protocols recommend setting the sonicator bath to 40 °C to facilitate the dissolution of Ox063. Under these conditions, a large amount of Ox063 is converted after a few minutes. The Arrhenius relationship allows us to determine an activation energy of 18 ± 2 kcal mol^{-1} for the esterification of the alcohol groups of Ox063 by pyruvic acid (Fig. 4). The esterification occurs far from the radical center; therefore, it is not expected to have a significant effect on the EPR spectrum. Moreover, we previously demonstrated that the esterification of alcohol groups with succinyl moieties has no significant effect on the EPR spectrum.[32] To verify this hypothesis, a sample with 5% remaining Ox063 and 95% of a mixture of pyruvate esters was diluted to 30 μM in PBS (10 mM, pH = 7) to avoid spin–spin broadening, and the X-band spectrum was recorded under nitrogen to avoid oxygen-induced line broadening. As expected, the spectrum exhibits a single narrow line peak with a linewidth of ~180 mG, identical to the spectrum of Ox063 (see Fig. S3†).[22] This result shows that all derivatives have very similar g-factors.

Finally, to verify that this observation was not limited to pyruvic acid, Ox063 was mixed with lactic acid, another widely

Table 1 Summary of the kinetic parameters for the esterification of Ox063 with pyruvic acid

Temperature (°C)	k obs (min^{-1})	$t_{1/2}$ (min)	k^a (s^{-1}, M^{-1})
20	0.011 ± 0.003	63 ± 17	$1.33 \times 10^{-5} \pm 0.36 \times 10^{-5}$
25	0.021 ± 0.003	33 ± 4	$2.48 \times 10^{-5} \pm 0.31 \times 10^{-5}$
30	0.030 ± 0.006	23 ± 5	$3.52 \times 10^{-5} \pm 0.73 \times 10^{-5}$
35	0.063 ± 0.023	12 ± 4	$7.36 \times 10^{-5} \pm 2.65 \times 10^{-5}$

[a] Calculated using [pyruvic acid] = 14.1 M.

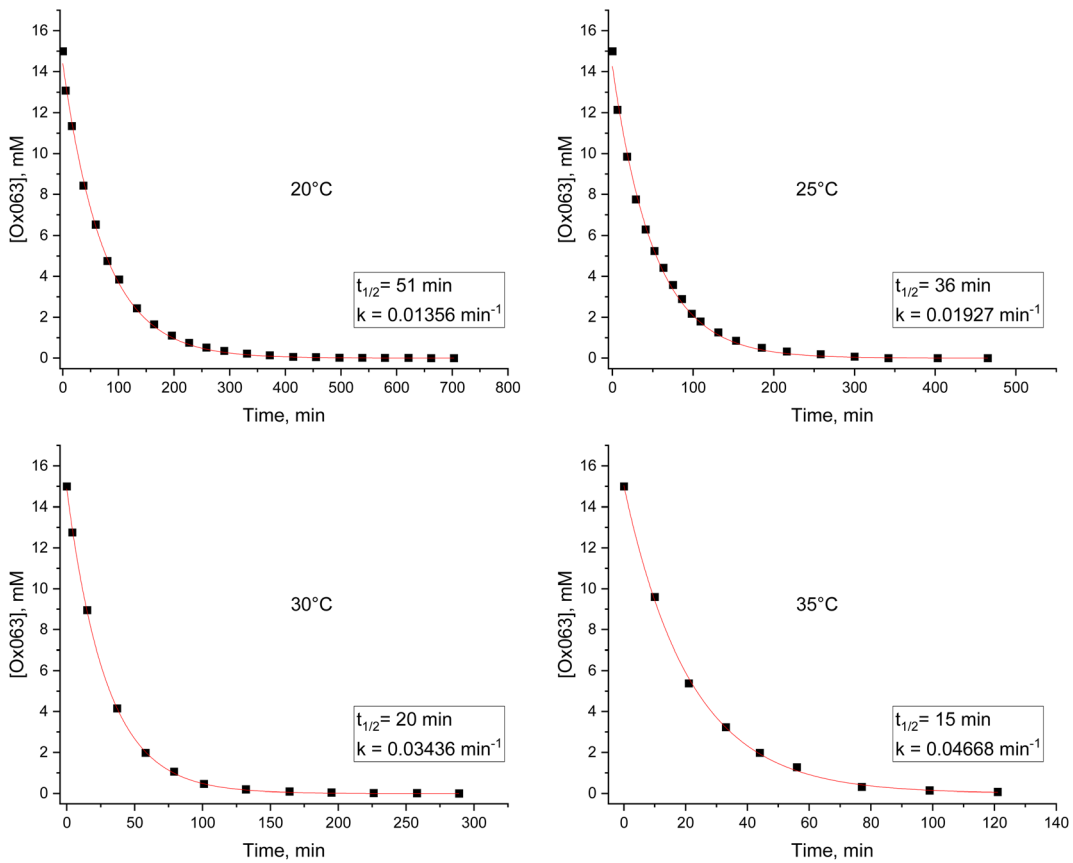

Fig. 3 Reaction kinetics of Ox063 in neat pyruvic acid at 20 °C, 25 °C, 30 °C, and 35 °C, followed by HPLC.

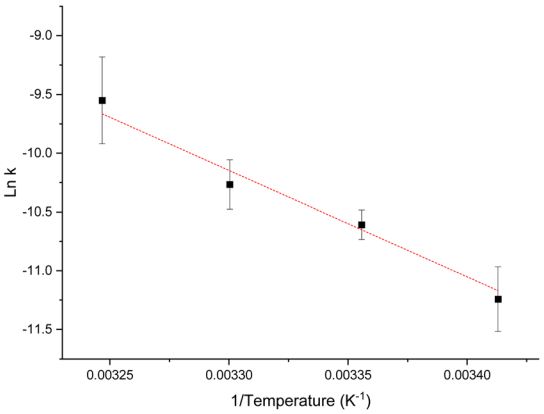

Fig. 4 Arrhenius plot for the determination of the activation energy for the esterification of one alcohol group of Ox063 by pyruvic acid, the slope as determined by the best fit was −9053.3 K. (see Fig. S2 and Table S1 for data points†).

used hyperpolarized probe. Similarly, lactate esters were formed using HPLC/MS (see Fig. S4†).

The primary aim of this study was to raise the attention of the DNP community on the potential chemical reactions occurring during the preparation of samples for DNP experiments. Chemical analysis of the functional groups present in the various constituents of the mixture should be carefully performed to anticipate and/or prevent these reactions. We demonstrated that when the popular OX063 PA is mixed with pyruvic acid or lactic acid, the alcohol functions undergo esterification at room temperature. Extra care is required when dissolving Ox063 in an organic carboxylic acid because it can lead to ester formation. To mitigate this reaction, the mixing temperature should be kept as low as possible, and the samples should be frozen immediately to stop the reaction. The use of carboxylate salts of ^{13}C-enriched metabolites could prevent this reaction.[33] Alternatively, the Ox063 analog, in which the alcohols have been methylated (OX063Me or AH111501, see Fig. S5 for structures†), is another popular PA used for metabolic imaging in clinical trials. This variant is protected by the reaction described here.

Data availability

All the data points for the kinetics and fitting parameters and data for the Arrhenius plot have been included in the ESI.†

Author contributions

BD designed the study. BD and MMH performed the experiment and analyzed the data. BD wrote the manuscript, and MMH edited the manuscript.

Conflicts of interest

None.

Acknowledgements

This study was partially funded by the National Institute of Health grant numbers R01EB032321, R21EB028553, and R21GM143595. The author thanks Martin Poncelet for his insight and the preliminary data.

References

1 Z. J. Wang, M. A. Ohliger, P. E. Z. Larson, J. W. Gordon, R. A. Bok, J. Slater, J. E. Villanueva-Meyer, C. P. Hess, J. Kurhanewicz and D. B. Vigneron, Hyperpolarized 13C MRI: State of the Art and Future Directions, *Radiology*, 2019, **291**(2), 273–284.
2 L. Lumata, Z. Kovacs, A. D. Sherry, C. Malloy, S. Hill, J. van Tol, L. Yu, L. Song and M. E. Merritt, Electron spin resonance studies of trityl OX063 at a concentration optimal for DNP, *Phys. Chem. Chem. Phys.*, 2013, **15**(24), 9800–9807.
3 S. J. Elliott, Q. Stern, M. Ceillier, T. El Daraï, S. F. Cousin, O. Cala and S. Jannin, Practical dissolution dynamic nuclear polarization, *Prog. Nucl. Magn. Reson. Spectrosc.*, 2021, **126–127**, 59–100.
4 J. H. Ardenkjaer-Larsen, On the present and future of dissolution-DNP, *J. Magn. Reson.*, 2016, **264**, 3–12.
5 J. Kurhanewicz, D. B. Vigneron, J. H. Ardenkjaer-Larsen, J. A. Bankson, K. Brindle, C. H. Cunningham, F. A. Gallagher, K. R. Keshari, A. Kjaer, C. Laustsen, *et al.*, Hyperpolarized (13)C MRI: Path to Clinical Translation in Oncology, *Neoplasia*, 2019, **21**(1), 1–16.
6 S. Ros, A. J. Wright, A. Bruna, C. Caldas and K. M. Brindle, Metabolic imaging with hyperpolarized [1-13C] pyruvate in patient-derived preclinical mouse models of breast cancer, *STAR Protoc.*, 2021, **2**(3), 100608.
7 S. Pudakalakatti, P. Raj, T. C. Salzillo, J. S. Enriquez, D. Bourgeois, P. Dutta, M. Titus, S. Shams, P. Bhosale, M. Kim, *et al.*, Metabolic Imaging Using Hyperpolarization for Assessment of Premalignancy, *Methods Mol. Biol.*, 2022, **2435**, 169–180.
8 B. T. Scroggins, M. Matsuo, A. O. White, K. Saito, J. P. Munasinghe, C. Sourbier, K. Yamamoto, V. Diaz, Y. Takakusagi, K. Ichikawa, *et al.*, Hyperpolarized [1-13C]-Pyruvate Magnetic Resonance Spectroscopic Imaging of Prostate Cancer *In Vivo* Predicts Efficacy of Targeting the Warburg Effect, *Clin. Cancer Res.*, 2018, **24**(13), 3137–3148.
9 E. Bliemsrieder, G. Kaissis, M. Grashei, G. Topping, J. Altomonte, C. Hundshammer, F. Lohöfer, I. Heid, D. Keim, S. Gebrekidan, *et al.*, Hyperpolarized 13C pyruvate magnetic resonance spectroscopy for *in vivo* metabolic phenotyping of rat HCC, *Sci. Rep.*, 2021, **11**(1), 1191.
10 E. M. Serrao, M. I. Kettunen, T. B. Rodrigues, D. Y. Lewis, F. A. Gallagher, D. E. Hu and K. M. Brindle, Analysis of 13C and 14C labeling in pyruvate and lactate in tumor and blood of lymphoma-bearing mice injected with 13C- and 14C-labeled pyruvate, *NMR Biomed.*, 2018, **31**(5), e3901.

11 E. Can, J. A. M. Bastiaansen, D.-L. Couturier, R. Gruetter, H. A. I. Yoshihara and A. Comment, [13C]bicarbonate labelled from hyperpolarized [1-13C]pyruvate is an *in vivo* marker of hepatic gluconeogenesis in fasted state, *Commun. Biol.*, 2022, **5**(1), 10.

12 K. Saito, S. Matsumoto, Y. Takakusagi, M. Matsuo, H. D. Morris, M. J. Lizak, J. P. Munasinghe, N. Devasahayam, S. Subramanian, J. B. Mitchell and M. C. Krishna, 13C-MR Spectroscopic Imaging with Hyperpolarized [1-13C]pyruvate Detects Early Response to Radiotherapy in SCC Tumors and HT-29 Tumors, *Clin. Cancer Res.*, 2015, **21**(22), 5073–5081.

13 N. T. Nguyen, O. N. M. D. Rasanjala and I. Park, Optimization of Scan Parameters for *in vivo* Hyperpolarized Carbon-13 Magnetic Resonance Spectroscopic Imaging, *Investig. Magn. Reson. Imaging*, 2022, **26**(2), 125–134.

14 M. Matsuo, T. Kawai, S. Kishimoto, K. Saito, J. Munasinghe, N. Devasahayam, J. B. Mitchell and M. C. Krishna, Co-imaging of the tumor oxygenation and metabolism using electron paramagnetic resonance imaging and 13-C hyperpolarized magnetic resonance imaging before and after irradiation, *Oncotarget*, 2018, **9**(38), 25089–25100.

15 S. Hu, H. A. I. Yoshihara, R. Bok, J. Zhou, M. Zhu, J. Kurhanewicz and D. B. Vigneron, Use of hyperpolarized [1-13C]pyruvate and [2-13C]pyruvate to probe the effects of the anticancer agent dichloroacetate on mitochondrial metabolism *in vivo* in the normal rat, *Magn. Reson. Imaging*, 2012, **30**(10), 1367–1372.

16 M. I. Menzel, E. V. Farrell, M. A. Janich, O. Khegai, F. Wiesinger, S. Nekolla, A. M. Otto, A. Haase, R. F. Schulte and M. Schwaiger, Multimodal Assessment of *In Vivo* Metabolism with Hyperpolarized [1-13C]MR Spectroscopy and 18F-FDG PET Imaging in Hepatocellular Carcinoma Tumor–Bearing Rats, *J. Nucl. Med.*, 2013, **54**(7), 1113–1119.

17 A. Flori, F. Frijia, V. Lionetti, J. H. Ardenkjaer-Larsen, V. Positano, G. Giovannetti, R. F. Schulte, F. Wiesinger, F. A. Recchia, L. Landini, *et al.*, DNP Methods for Cardiac Metabolic Imaging with Hyperpolarized [1-13C]pyruvate Large Dose Injection in Pigs, *Appl. Magn. Reson.*, 2012, **43**(1), 299–310.

18 V. Ruiz-Rodado, T. M. Malta, T. Seki, A. Lita, T. Dowdy, O. Celiku, A. Cavazos-Saldana, A. Li, Y. Liu, S. Han, *et al.*, Metabolic reprogramming associated with aggressiveness occurs in the G-CIMP-high molecular subtypes of IDH1mut lower grade gliomas, *Neuro-Oncology*, 2019, **22**(4), 480–492.

19 H. J. Atherton, M. A. Schroeder, M. S. Dodd, L. C. Heather, E. E. Carter, L. E. Cochlin, S. Nagel, N. R. Sibson, G. K. Radda, K. Clarke and D. J. Tyler, Validation of the *in vivo* assessment of pyruvate dehydrogenase activity using hyperpolarised 13C MRS, *NMR Biomed.*, 2011, **24**(2), 201–208.

20 L. Lampp, O. Y. Rogozhnikova, D. V. Trukhin, V. M. Tormyshev, M. K. Bowman, N. Devasahayam, M. C. Krishna, K. Mader and P. Imming, A radical containing injectable in-situ-oleogel and emulgel for prolonged in-vivo oxygen measurements with CW EPR, *Free Radical Biol. Med.*, 2019, **130**, 120–127.

21 M. Serda, Y. K. Wu, E. D. Barth, H. J. Halpern and V. H. Rawal, EPR Imaging Spin Probe Trityl Radical OX063: A Method for Its Isolation from Animal Effluent, Redox Chemistry of Its Quinone Methide Oxidation Product, and *in Vivo* Application in a Mouse, *Chem. Res. Toxicol.*, 2016, **29**(12), 2153–2156.

22 K.-i. Matsumoto, S. English, J. Yoo, K.-i. Yamada, N. Devasahayam, J. A. Cook, J. B. Mitchell, S. Subramanian and M. C. Krishna, Pharmacokinetics of a triarylmethyl-type paramagnetic spin probe used in EPR oximetry, *Magn. Reson. Med.*, 2004, **52**(4), 885–892.

23 K.-i. Matsumoto, F. Hyodo, J. B. Mitchell and M. C. Krishna, Effect of body temperature on the pharmacokinetics of a triarylmethyl-type paramagnetic contrast agent used in EPR oximetry, *Magn. Reson. Med.*, 2018, **79**(2), 1212–1218.

24 B. Epel, N. Viswakarma, S. V. Sundramoorthy, N. J. Pawar and M. Kotecha, Oxygen Imaging of a Rabbit Tumor Using a Human-Sized Pulse Electron Paramagnetic Resonance Imager, *Mol. Imaging Biol.*, 2024, **26**(3), 403–410.

25 S. Kishimoto, K. Horie, N. Devasahayam, K. Yamashita, C. Gadisetti, K. Yamamoto, J. R. Brender, J. B. Mitchell, M. C. Krishna, W. M. Linehan and D. R. Crooks, Low Field Magnetic Resonance Imaging to Detect Acute Kidney Injury, *bioRxiv*, 2025, preprint, 2025.01.22.634393, DOI: 10.1101/2025.01.22.634393.

26 L. Lumata, M. E. Merritt, Z. Hashami, S. J. Ratnakar and Z. Kovacs, Production and NMR Characterization of Hyperpolarized 107,109Ag Complexes, *Angew. Chem., Int. Ed.*, 2012, **51**(2), 525–527.

27 A. Equbal, Y. Li, T. Tabassum and S. Han, Crossover from a Solid Effect to Thermal Mixing 1H Dynamic Nuclear Polarization with Trityl-OX063, *J. Phys. Chem. Lett.*, 2020, **11**(9), 3718–3723.

28 M. Poncelet, J. L. Huffman, V. V. Khramtsov, I. Dhimitruka and B. Driesschaert, Synthesis of hydroxyethyl tetrathiatriarylmethyl radicals OX063 and OX071, *RSC Adv.*, 2019, **9**(60), 35073–35076.

29 T. D. Gluth, M. Poncelet, M. Gencheva, E. H. Hoblitzell, V. V. Khramtsov, T. D. Eubank and B. Driesschaert, Biocompatible Monophosphonated Trityl Spin Probe, HOPE71, for *In Vivo* Measurement of pO2, pH, and [Pi] by Electron Paramagnetic Resonance Spectroscopy, *Anal. Chem.*, 2023, **95**(2), 946–954.

30 M. Poncelet, T. Ngendahimana, T. D. Gluth, E. H. Hoblitzell, T. D. Eubank, G. R. Eaton, S. S. Eaton and B. Driesschaert, Synthesis and characterization of a biocompatible 13C1 isotopologue of trityl radical OX071 for *in vivo* EPR viscometry, *Analyst*, 2022, **147**(24), 5643–5648.

31 F. Jähnig, G. Kwiatkowski, A. Däpp, A. Hunkeler, B. H. Meier, S. Kozerke and M. Ernst, Dissolution DNP using trityl radicals at 7 T field, *Phys. Chem. Chem. Phys.*, 2017, **19**(29), 19196–19204.

32 M. A. Shaw, M. Poncelet, N. Viswakarma, G. P. Vallerini, S. Hameed, T. D. Gluth, W. J. Geldenhuys, E. H. Hoblitzell, T. D. Eubank, B. Epel, *et al.*, SOX71, A Biocompatible

Succinyl Derivative of the Triarylmethyl Radical OX071 for *In Vivo* Quantitative Oxygen Mapping Using Electron Paramagnetic Resonance, *Mol. Imaging Biol.*, 2024, **26**(3), 542–552.

33 L. Lumata, M. E. Merritt, C. R. Malloy, A. D. Sherry and Z. Kovacs, Impact of Gd3+ on DNP of [1-13C]Pyruvate Doped with Trityl OX063, BDPA, or 4-Oxo-TEMPO, *J. Phys. Chem. A*, 2012, **116**(21), 5129–5138.